Elementary Excitations in Crystalline Matter: Phonons and Magnons

K. Schmalzl

Manuel Angst, Thomas Brückel, Dieter Richter, Reiner Zorn (Eds.):
Scattering Methods for Condensed Matter Research: Towards Novel Applications at Future Sources
Lecture Notes of the 43rd IFF Spring School 2012
Schriften des Forschungszentrums Jülich / Reihe Schlüsseltechnologien / Key Technologies, Vol. 33
JCNS, PGI, ICS, IAS

Forschungszentrum Jülich GmbH, JCNS, PGI, ICS, IAS, 2012
ISBN: 978-3-89336-759-7

B 4 Elementary Excitations in Crystalline Matter: Phonons and Magnons [1]

K. Schmalzl

Jülich Centre for Neutron Science

Forschungszentrum Jülich GmbH

Contents

---

[1] Lecture Notes of the 43$^{\mathrm{rd}}$ IFF Spring School "Scattering Methods for Condensed Matter Research: Towards Novel Applications at Future Sources" (Forschungszentrum Jülich, 2012). All rights reserved.

1 Introduction

Any kind of matter can be seen as a system of interacting particles, where the structure is determined by its ground state and the dynamics is represented by excited states. Ground states and excited states are determined by the Coulomb interaction between ions and electrons. Due to this interaction the excited states are collective excitations.

Dynamical properties of matter are directly related to physical properties, which on their part can be measured in experiments. To understand phenomena like temperature dependent effects, superconductivity, phase transition or also magnetic properties, to name just a few, the basic elementary excitations have to be understood.

In this chapter two types of elementary excitations in matter will be discussed. First the concept of lattice waves in the harmonic approximation will be introduced. An outlook to anharmonic effects which lead to temperature dependent phenomena, and a short comparison to excitations in amorphous media will then be given.

Analogous to the periodic sequence of atoms in a lattice, the periodic arrangement of electronic spins of atoms leads to spin waves. On the basis of a model Hamiltonian the examples of ferro- and antiferromagnetism will be treated. The quasiparticle of the spin waves are the magnons, similar to the phonons for the lattice waves.

The main part of the formalism presented here deals with an infinite periodic system. As interactions in matter can be manifold and complicated appropriate approximations will be presented.

2 Lattice Excitations: Phonons

2.1 Adiabatic Approximation

A solid represents a quantum mechanical many-body system consisting of interacting nuclei and electrons. The Hamiltonian contains the kinetic and potential energy with all nuclear and electronic coordinates and momenta and their interaction.

$$H = H_{\mathrm{nucl}} + H_{\mathrm{el}} + H_{\mathrm{el-nucl}}.$$

The wavefunction is thus a function of all nuclear, electronic, and spin coordinates. As this is a rather complicated system in total, approximations are needed: With the adiabatic approximation (also called Born-Oppenheimer approximation) one can decouple the electron from the nuclear dynamics: One uses the fact that the light electrons adjust instantaneously to the slower motion of the heavy ionic cores (with the electron mass being about 10^{-4} of the ion mass!). During the motion of the atomic cores the electrons follow the ions adiabatically and remain in their ground state, the energy of which, however, is given by the ionic configuration.

2.2 Harmonic Approximation

The ions move in a potential V, made up of the potential energy of the ion configuration and of the energy of the electrons in this configuration.

Assuming small atomic displacements $\mathbf{u}_l$ out of their equilibrium positions, the potential energy V can be written as a Taylor series in these atomic displacements, and the Hamiltonian reads

$$H_{\mathrm{ion}} = \sum_l \frac{\mathbf{p}_l^2}{2m_l} + V_0 + \sum_{l,\alpha} \frac{\partial V}{\partial u_{l,\alpha}} u_{l,\alpha} + \frac{1}{2} \sum_{l,\alpha} \sum_{l',\beta} \frac{\partial^2 V}{\partial u_{l,\alpha} \partial u_{l',\beta}} u_{l,\alpha} u_{l',\beta} + \dots . \tag{1}$$

If one neglects all terms higher than of second order, indicated by dots, this approximation is called the harmonic approximation. (This approximation is made for convenience: the harmonic equations of motions are easier to solve and this approximation is justified as the harmonic term is the dominant one and gives good results at least at low temperatures.)
A closer look at equation (1) shows: V_0 is a constant and not relevant for the dynamics. The first-order term vanishes since it is assumed that the particles vibrate around their equilibrium positions:

$$H_{\text{ion}} = \sum_l \frac{\mathbf{p}_l^2}{2m_l} + \frac{1}{2}\sum_{l,\alpha}\sum_{l',\beta} \frac{\partial^2 V}{\partial u_{l,\alpha}\partial u_{l',\beta}} u_{l,\alpha} u_{l'\beta}. \tag{2}$$

The second-order derivatives of the potential are the force constants

$$\Phi_{\alpha\beta}(ll') = \frac{\partial^2 V}{\partial u_{l,\alpha}\partial u_{l',\beta}}. \tag{3}$$

They describe the force acting on the atom l in the direction α when the atom l' is displaced in the direction β.
In the harmonic approximation, the atomic vibrations can be transformed into decoupled normal vibrations (as we see later, leading for periodic systems to (harmonic) phonon dispersion curves). As these latter vibrations have no coupling, they have infinite lifetime. For lifetime (linewidth) or frequency shift and other temperature effects one would have to consider the higher-order terms neglected in the harmonic approximation. They are called the anharmonic terms.
The considerations above apply to crystalline as well as amorphous solids.

2.3 Normal Coordinates and Phonons

To finally investigate vibrations of particles in our system we have to solve the equations of motion,

$$m\frac{\partial^2 u_{l,\alpha}}{\partial t^2} = -\frac{\partial V}{\partial u_{l,\alpha}} = -\sum_{l',\beta} \Phi_{\alpha\beta}(ll') u_{l',\beta}.$$

Because of the harmonic approximation we can formulate a harmonic ansatz for the time dependence of the displacements $\mathbf{u}$ for all l,

$$\mathbf{u}_l \propto \exp(-i\omega t) \tag{4}$$

and get as result

$$\sum_{l',\beta} \left(\Phi_{\alpha\beta}(ll') - \omega^2 m_l \delta_{l,l'}\delta_{\alpha,\beta}\right) u_{l',\beta} = 0\,. \tag{5}$$

The sum runs over all atoms in the system. With N atoms, this is a $3N \times 3N$-dimensional problem resulting in a $3N \times 3N$ force-constant matrix.
After diagonalizing this matrix, the diagonal elements are the squared frequencies. All eigenfrequencies ω_λ are represented by eigenvectors $\chi(l, \alpha|\lambda)$ with quantum numbers λ, and the general solution is

$$u_{l,\alpha}(t) = \sum_\lambda Q_\lambda \chi(l, \alpha|\lambda) e^{-i\omega_\lambda t}\,. \tag{6}$$

The superposition coefficients Q_λ are the so-called normal coordinates.

Upon quantization, the normal coordinates can be expressed in terms of phonon annihilation and creation operators, $a_\lambda, a_\lambda^\dagger$,

$$Q_\lambda \to \sqrt{\hbar/2\omega_\lambda}\left(a_\lambda + a_\lambda^\dagger\right). \tag{7}$$

With the eigensolutions we can also formulate the Hamiltonian (1) in terms of these solutions or normal coordinates. In this representation the Hamiltonian will then be a set of uncoupled harmonic oscillators, where each of them corresponds to a collective mode. This decoupling is possible only within the harmonic approximation,

$$H = \sum_\lambda \hbar\omega_\lambda \left(n_\lambda + \tfrac{1}{2}\right) \tag{8}$$

with $\frac{1}{2}\hbar\omega$ being the lowest energy state of a quantum harmonic oscillator and

$$n_\lambda = a_\lambda^\dagger a_\lambda \tag{9}$$

the occupation number operator with the commutation relations for creation and annihilation operators, $[a_\lambda, a_{\lambda'}^\dagger] = \delta_{\lambda,\lambda'}$, $[a_\lambda, a_{\lambda'}] = 0 = [a_\lambda^\dagger, a_{\lambda'}^\dagger]$; $\hbar\omega_\lambda$ is the excitation energy quantum of the collective mode, the phonon energy.

2.4 Bloch's Theorem and Vibrations in Crystals

A crystal is an infinite periodic system, and with Bloch's theorem (or mathematically Floquet's theorem) we can make use of this lattice periodicity. The theorem states that the displacements of same atoms in different unit cells differ only by a phase factor. We denote now not only the elementary cell by an index l but also the atom within a cell by an index κ. Then the displacements u can be written as

$$\mathbf{u}(l\kappa) = \frac{1}{\sqrt{m_\kappa}}\mathbf{e}(\kappa|\mathbf{q})e^{i\mathbf{q}\cdot\mathbf{R}_l}. \tag{10}$$

(The mass factor is for later convenience.) The first part describes the periodicity of the cells, the second one is the wave-like part.
Now the equation of motion takes the form

$$\omega^2(\mathbf{q})e_\alpha(\kappa|\mathbf{q}) = \sum_{\kappa',\beta} D_{\alpha\beta}(\kappa\kappa'|\mathbf{q})e_\beta(\kappa'|\mathbf{q}). \tag{11}$$

This equation now treats only atoms within one unit cell. The so-called dynamical matrix $D_{\kappa\kappa'}(\mathbf{q})$ is the Fourier transform of the force constant matrix (3), multiplied by the square root of the masses of the atoms (in order for (11) to obtain the normal form of an eigenvalue equation),

$$D_{\alpha\beta}(\kappa\kappa'|\mathbf{q}) = \frac{1}{\sqrt{m_\kappa m_{\kappa'}}}\sum_{l'} \Phi_{\alpha\beta}(l,\kappa,l',\kappa')e^{i\mathbf{q}\cdot(\mathbf{R}_{l'}-\mathbf{R}_l)} \tag{12}$$

(D-definition after Maradudin et al. [2]).
If r is the number of atoms in the elementary cell, now the $3N \times 3N$ problem of (5) is reduced to a $3r \times 3r$ problem in (11). For each wavevector $\mathbf{q}$ the secular problem

$$\left|D_{\alpha\beta}(\kappa\kappa'|\mathbf{q}) - \omega^2(\mathbf{q})\delta_{\alpha,\beta}\delta_{\kappa,\kappa'}\right| = 0 \tag{13}$$

has to be solved. The diagonalization of the dynamical matrix leads to the eigenfrequencies $\omega_j(\mathbf{q})$ with the branch index j. The quantum number λ for general systems above is now detailed by two quantum numbers $\mathbf{q}$ and j for lattices. For each eigenfrequency $\omega_j(\mathbf{q}) = \omega_j(-\mathbf{q})$ with $j = 1, \ldots, 3r$ a corresponding eigenvector $\mathbf{e}(\kappa|\mathbf{q}, j)$ to equation (11) exists.

As we have seen we can gain all phonon properties from considering only one unit cell. In the same way as a crystal is composed of a periodic array of unit cells also the phonon properties show a periodicity:

$$\omega_j(\mathbf{q}) = \omega_j(\mathbf{q} + \tau),$$
$$\mathbf{e}(\kappa|\mathbf{q}, j) = \mathbf{e}(\kappa|\mathbf{q} + \tau, j)\,.$$

The vector τ is a so-called reciprocal-lattice vector.
But still in an experiment one would not necessarily find the same result in different Brillouin zones (different τ): the scattering function contains terms involving

$$(\mathbf{q} + \tau) \cdot \mathbf{e}(\kappa|\mathbf{q}, j) e^{i(\mathbf{q}+\tau)\cdot\mathbf{R}(\kappa)},$$

which might lead to different scattering intensities in different Brillouin zones for the same frequency!
Because of the hermiticity of the matrix the squared frequencies $\omega_j^2(\mathbf{q})$ must be real, and with this $\omega_j(\mathbf{q})$ can be either real or imaginary. In the latter case, for a calculated imaginary frequency, the crystal shows an instability. The curves $\omega_j(\mathbf{q})$ as a function of q for a given direction of $\mathbf{q}$ are called dispersion curves (analogous to the band-structure curves in the electronic case). The solutions of equation (11) or (13) describe collective modes for which all ions in a lattice move with the same time dependence but with a phase shift with respect to each other. The eigenvectors form a complete set of solutions that can be used as basis for any arbitrary motion of the ions.
With r atoms in the unit cell we will find $3r$ phonon branches per $\mathbf{q}$-vector. The factor 3 describes thereby the three spatial degrees of freedom of each atom within the elementary cell. Common to the phonon dispersion of all solids are the branches with lowest frequencies, which are the acoustic modes which start from the center of the Brillouin zone with a linear dependence on q. A simple picture of acoustic modes can be drawn with one of the simplest models, the monatomic linear chain.

2.5 Phonon Dispersion Curves

Consider a linear chain with atoms, all with mass M, separated by the unit cell length a. And assume an average force constant C acting between neighboring planes. This is the model of a monatomic linear chain. Let U_i be the displacement of plane i, With the periodic time dependence $U_i(t) = u_i e^{-i\omega t}$ the equations of motion (5) reduce to

$$-M\omega^2 u_i = C(u_{i+1} + u_{i-1} - 2u_i)\,.$$

The solution of these equations are plane waves $u_{i\pm 1} = u_i e^{\pm iqa}$ periodic with wavevector q. For the dispersion relation $\omega(q)$ of the monatomic linear chain we get:

$$\omega(q) = (4C/M)^{1/2} |\sin\frac{qa}{2}|.$$

This dispersion is schematically shown in fig. 1. For one atom in one dimension we will get only one phonon branch. The sine dependence shows us: For small q-vectors (long wavelengths) the

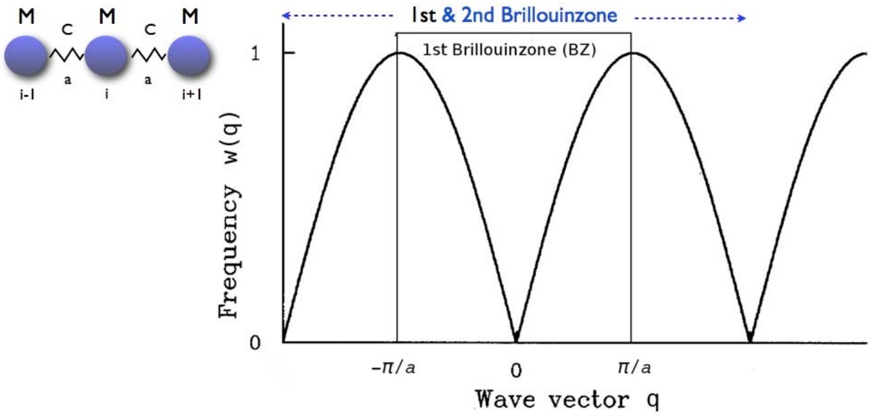

Fig. 1: *Schematic representation of the dispersion curve of the monatomic linear chain. The phonon dispersion can be limited to the first Brillouin zone.*

frequency ω is linear in q, $\omega = c_s q$ with the velocity of sound c_s. Also we see: for small q-vectors $q \to 0$ the frequency tends to zero, $\omega \to 0$.
One striking feature is the periodicity of the function: the period is $2\pi/a$, which is equal to a unit cell length in reciprocal space. We have seen already that one can add a reciprocal lattice vector $\tau = 2\pi/a$ to any point at any wavevector, the frequency and equations of motion will be identical to the first one. All information is contained within $-\pi/a < q < \pi/a$. This range is called the first Brillouin zone. Further zones are called the second, third, etc. Brillouin zone. One can limit the phonon dispersion to the first Brillouin zone.
The values $q = \pm\frac{\pi}{a}$ are the Brillouin zone boundaries lying half way between centers. In our case the slope of the dispersion is zero at the zone boundary, $d\omega/dq = 0$ for $q = \pm\frac{\pi}{a}$.

Phonon modes are grouped in acoustic and optic. Of the $3r$ possible modes, three modes are acoustic, and the remaining $(3r - 3)$ modes are optic with a a non-zero frequency at $\mathbf{q} = 0$.
In the acoustic modes in the long-wavelength limit $q \to 0$ all atoms move with nearly the same phase. The wavelength λ of this movement is much larger than the lattice constant a. Depending

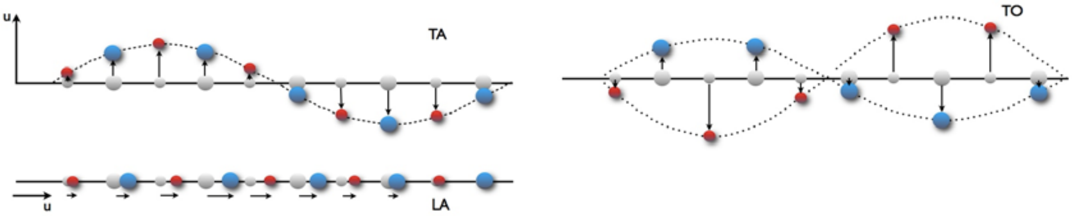

Fig. 2: *Schematic displacement patterns for a two-atomic linear chain for* $\mathbf{q} \neq 0$. *Top left:transverse acoustic mode (TA), bottom left: longitudinal acoustic mode (LA). Right: transverse optic mode (TO).*

on the orientation of the polarization vectors $\mathbf{e}(\kappa|\mathbf{q}j)$ with respect to $\mathbf{q}$, the modes can possibly be further classified to be longitudinal or transverse. In the longitudinal mode the displacement is parallel to the $\mathbf{q}$-vector, whereas in the two transverse modes the displacement is perpendicular. This may be true, however, only in main symmetry directions, e.g., for cubic symmetries along [100], [110], or [111] (edge, face, or space diagonal). In more complicated structures or away from main symmetry directions the modes show a mixture of these displacement patterns and cannot be classified as purely longitudinal or transverse movements anymore.

Phonon dispersion curves $\omega_j(\mathbf{q})$ are usually plotted along high-symmetry directions where degeneracies may occur. They are obtained experimentally, e.g., from inelastic scattering of neutrons, photons, or atoms, and theoretically, e.g., from model or ab initio calculations. For crystals of the same symmetry group similar dispersion curves are obtained, the details depending upon the specific atom masses and force constants. Scales for frequencies are typically $10^{12}\,\mathrm{s}^{-1}$ (THz) $\equiv 33.36\,\mathrm{cm}^{-1} \equiv 4.136\,\mathrm{meV}$.

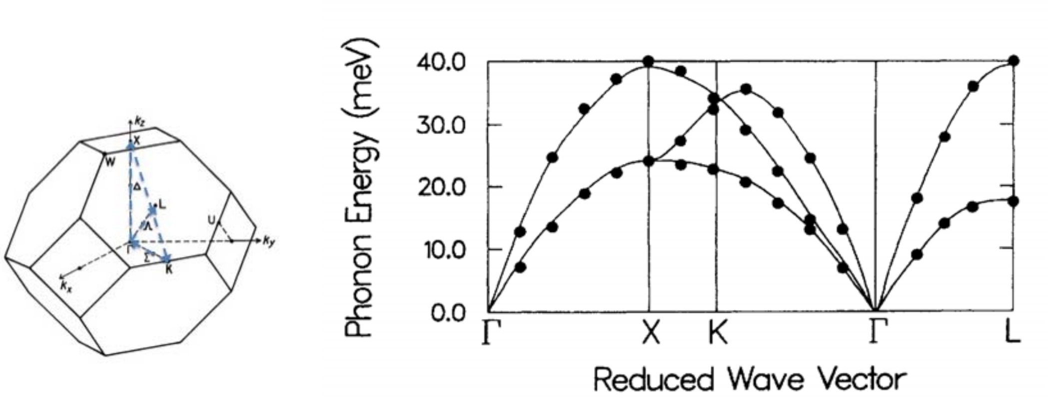

Fig. 3: *Phonon dispersion for aluminium from first principle ab initio methods in comparison with data from inelastic neutron scattering. [3] Left: Brillouin zone of the fcc lattice with the measured high symmetry directions marked.*

Figure 3 shows the phonon dispersion curve for the example of aluminium along the main symmetry directions of the fcc Brillouin zone. With one atom in the primitive unit cell the phonon dispersion shows three acoustic branches (one LA, two TA). The two lower transverse acoustic branches are degenerate in $\Gamma - X$ and $\Gamma - L$-direction which is characteristic of the symmetry group (Fm3m) of fcc aluminium. Also can be seen that the modes show zero curvature at the zone boundaries.

With two and more atoms in the unit cell the dispersion will show also optic modes. In ionic crystals these modes may be dipole-active, depending on the involved atoms, and can then be excited optically, e.g., by infra-red light (therefore they are called optic modes).

Figure 4 shows an example for a phonon dispersion with three atoms per unit cell, $\mathrm{CaF_2}$, along the three main symmetry directions of the fcc Brillouin zone and along several other directions along the Brillouin zone faces. Depicted are also the group-symmetrical representations of the different phonon branches.

In ionic crystals where the different atoms are (differently) charged a macroscopic longitudinal electric field is introduced with the displacement of the atoms. As this field is of longitudinal character, longitudinal optic modes at $q = 0$ couple to this field and their energy is increased, whereas transverse modes are not affected. This fact is described by the Lyddane-Sachs-Teller relation for ionic crystals for long wavelengths:

$$\frac{\epsilon(0)}{\epsilon_\infty} = \frac{\omega_L^2}{\omega_T^2}.$$

This means, in ionic crystals the degeneracy is partly removed at the Brillouin zone center for

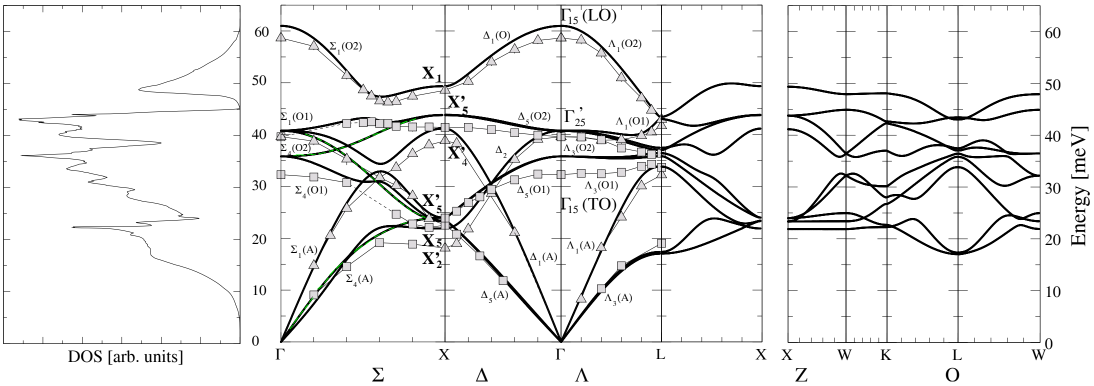

Fig. 4: *DOS and phonon dispersion curves for CaF_2 from inelastic neutron scattering (symbols) and ab initio method. [4] Triangles mean phonons measured in longitudinal, squares in transverse polarization.*

optic modes. The LO modes have higher frequencies than the TO modes. This LO–TO splitting might be anisotropic and direction-dependent.
For identical atoms in the unit cell, the modes at the Brillouin zone center are degenerate. With increasing charge difference the gap between the LO and TO modes increases.

2.6 Phonon Density of States

A convenient way to display a phonon spectrum is also the phonon density of states (DOS). The phonon spectrum with a a given dispersion $\omega_j(\mathbf{q})$ can be characterized by the one-phonon density of states, $D(\omega) = \sum_{\mathbf{q},j} \delta(\omega - \omega_j(\mathbf{q}))$. It counts the number of phonon modes within a frequency interval at a given frequency ω by summing over all branches in the first Brillouin zone and is the sum of all frequencies in all directions in reciprocal space (not only those in a chosen dispersion direction). It is shown on the left hand side of fig. 4. Pronounced peaks can be seen coming from flat parts of the branches.

2.7 Anharmonic Effects and Phase Transitions

Within the harmonic approximation we introduced before many experimental results can be reproduced but temperature dependent effects cannot be predicted. In experiment and real life those effects are omnipresent. To model and understand effects like thermal expansion, effects coming from phonon-phonon collision or phase transitions, etc., the higher order terms in the Hamiltonian (1) have to be taken into account. With this the decoupling of vibrations is not possible anymore and an interaction of phonons takes place.
In experiment temperature effects will be seen in a shift of the phonon frequency compared to the harmonic one, in thermal expansion and a phonon linewidth broadening. The linewidth is the inverse of the lifetime of a phonon and can be seen via a damping of the spectral lines in experiment. This is ascribed to decay processes where a phonon decays after a certain time into other phonon states.
The thermal expansion is the process easiest to consider. With increasing temperature in general the volume of the material increases. One can expect that frequencies decrease with increasing volume as bond lengths increase and interatomic forces decrease.

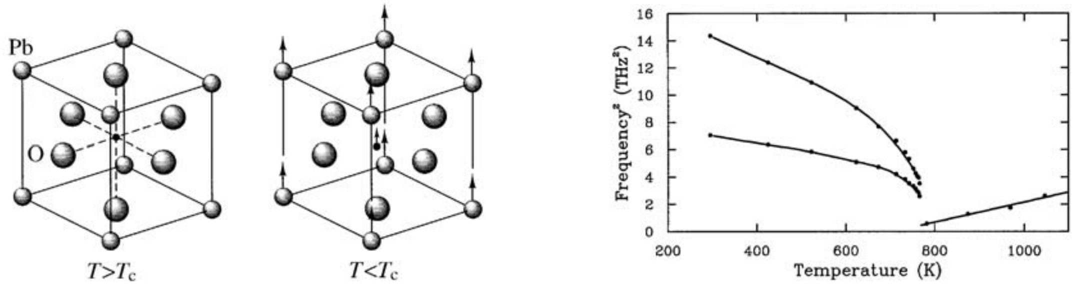

Fig. 5: *PbTiO$_3$ undergoes a cubic-tetragonal phase transition at 763 K. Left: distortion associated with the transition involves small atomic displacements in [001]. Right: Decreasing frequency when approaching the transition temperature. Below the phase transition a splitting in two modes occurs. Taken from [5])*

The change of volume and frequency with changing temperature can be described with the mode-Grüneisen-parameter:

$$\gamma_{\mathbf{q},j} = -\frac{\partial \ln \omega(\mathbf{q}, j)}{\partial(\ln V)}.$$

For the shift of phonon frequencies decay and scattering processes have to be taken into account, including higher order terms than the harmonic ones as well as thermal expansion, all depending on higher order terms in the potential.

When calculating the phonon frequencies of the structure known to exist at high temperatures with the harmonic equations of motion (11), the squared phonon frequencies ω^2 can be negative, leading to imaginary frequencies. This means the assumed structure is not stable at 0 K and an another structure with lower energy exists. The structural distortion can be identified when finding the eigenvector corresponding to the imaginary frequency.

An example for the change of frequency with temperature is the second order displacive phase transition. From high to low temperatures the system seems to undergo small structural modifications. Figure 5 shows the temperature variation of the two-fold degenerate TO frequency near the ferroelectric phase transition in PbTiO$_3$. When cooling in an experiment from high to low temperatures the phonon frequency will decrease from the stable harmonic value at high temperatures to zero at the transition. At this point the crystal is unstable against the corresponding distortion and undergoes a phase transition to a lower energy phase. This mode which can be found in the high temperature phase is called a soft mode. Below the phase transition there will be another mode increasing in frequency when cooling. Below T_c a splitting into two modes occurs due to the reduced symmetry.

2.8 Other Thermal Effects

The internal energy of a phonon system is

$$U(T) = \sum_{\mathbf{q},j} \hbar\omega_j(\mathbf{q} \left(\langle n_{\mathbf{q},j}\rangle + \tfrac{1}{2}\right) \tag{14}$$

with the Bose occupation number

$$\langle n_{\mathbf{q},j}\rangle = \frac{1}{1 - e^{\hbar\omega_j(\mathbf{q})/k_B T}}. \tag{15}$$

There are two effects from temperature: The one comes from the explicit T-dependence of the Bose factor; the other comes from the (anharmonic) T-dependence of $\omega_j(\mathbf{q})$. Neglecting the latter is called the quasi-harmonic approximation.
Similarly to the internal energy the entropy, free energy, specific heat, etc. can be calculated.

2.9 Amorphous Media and Liquids

So far we considered perfect lattice symmetries.
If only single atoms of the crystal are replaced by defects, then still an average lattice periodicity on a long-range scale is preserved. The wavevectors are still approximately good quantum numbers, and the notions of Brillouin zone etc. are good approximations. In contrast, in disordered materials like amorphous materials, glasses or liquids there is less or no long-range order at all leading to structural disorder. As a consequence, the $\mathbf{q}$-vector is not well defined and no longer a good quantum number.

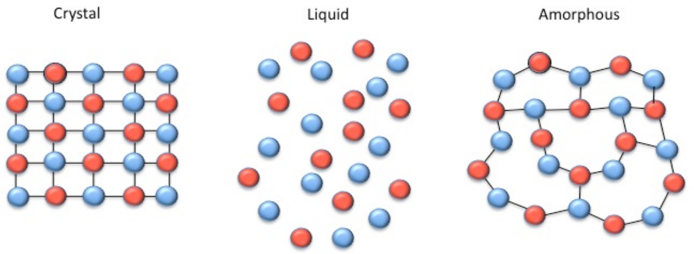

Fig. 6: *Schematic presentation of a crystalline, liquid and amorphous ordering. No long-range order or large distance periodicity exists in the latter two.*

But there exists still short range order and the local environment of a given atom is, similar to the crystalline case with nearest and next-nearest neighbor distances, relevant. With increasing distance from a given atom, these structural quantities are less well defined and become increasingly smeared out. With this loss of periodicity also no well defined Brillouin zones can be identified, one speaks about pseudo-Brillouin zones, where the size of the zones is defined by the next neighbor distance.
Nevertheless, in the long-wavelength limit glasses and disordered materials behave like crystals with propagation of sound waves. In this limit the phonon dispersion is similar to the one found in a crystalline system. With increasing wavelength vibrational properties lose their plane-wave character, which can be seen as a broadening of spectral distribution in experiment coming from the disorder of the system. This means for small q a linear dispersion can be found which is the macroscopic velocity of sound in the system and corresponds to the longitudinal acoustic phonon branch.
Figure 7 shows measured longitudinal dispersion curves for different glass systems. The modes show a pseudo-periodic behavior, where the extent of the Brillouin zone is determined by the nearest neighbor distance. Depending on the system, the minimum in the second Brillouin zone, which would correspond to the next Brillouin zone center, might be more pronounced like it is in the case of ethanol hinting to an order at slightly larger length scales. Liquids and amorphous materials are different from crystalline systems in that the former have strongly reduced transverse forces. Anyway, for reduced symmetries the terms longitudinal and transverse might lose their meaning.

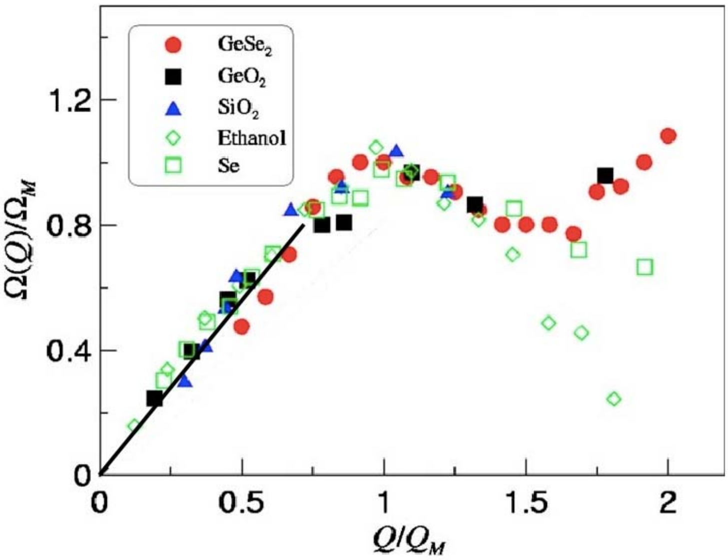

Fig. 7: *Dispersion curves of various glass-like systems measured with inelastic neutron scattering, rescaled for comparison in respect to frequency and wavevector Q [6]. The straight line indicates the velocity of sound.*

As a result of structural disorder, e.g., the heat conduction will be smaller in glasses and liquids than in crystalline materials due to defect-induced scattering. In a simple model, the heat conduction is given by

$$\kappa = \frac{1}{3} c_V v l$$

with the specific heat c_V, velocity v and mean free path length l. The structural or compositional disorder reduces the average mean free path and the thermal conductivity becomes reduced in comparison with that of a perfect crystal lattice.

3 Spin Waves: Magnons

So far we considered lattice vibrations, where the position of the atoms changes periodically leading to phonons as quantized particles. We will focus now on properties coming from the electron spin, which have been neglected so far. An electron system with its quantum-mechanical exchange interaction will lead to a spin-ordered ground state and its elementary excitations, the spin waves. The elementary excitations of a periodic spin system are of a wavelike character in analogy to lattice vibrations, and, similarly to the phonons, magnons as quantized particles of the spin wave, can be introduced. In this chapter the equation for spin wave excitations in a ferromagnet as well as in an antiferromagnet will be deduced. Usually magnetic order exists below a critical temperature at which a phase transition takes place. The temperature and magnetic field dependence will be treated shortly at the end of this chapter.

For the spin ordered ground state one can imagine different realizations, like all spins parallel (ferromagnetism), or antiparallel (antiferromagnetism), (anti-) ferrimagnetic ordering or more complex like helix-form.

Here we will focus on the most prominent cases of a spin ordering with parallel and antiparallel spins, leading to ferro- and antiferromagnetism.

$$\mathrm{FM}: \ldots \uparrow\uparrow\uparrow\uparrow\uparrow\uparrow\uparrow \ldots \qquad \mathrm{AFM}: \ldots \uparrow\downarrow\uparrow\downarrow\uparrow\downarrow\uparrow \ldots$$

Fig. 8: *Classical ferromagnetic (FM) and antiferromagnetic (AFM) ground state in a Heisenberg chain. The spin states* S_i^z*=+S and* S_i^z*=-S are pictured by '↑' and '↓'. The AFM ordering is described by two sublattices with opposite magnetization.*

The exchange interaction between magnetic moments leads to the alignment of the spins. The energy of the interaction between two atoms i and j and their spins $\mathbf{S}_i$ and $\mathbf{S}_j$ can be formulated within the Heisenberg model:

$$U = -2 \sum_{ij}{}' J_{ij} \mathbf{S}_i \cdot \mathbf{S}_j,$$

where J_{ij} is the exchange integral describing the exchange energy of overlapping charge distributions of the different atoms i and j. $\sum'$ means summation over $i \neq j$. For a ferromagnetic system the exchange integral is defined as positive, $J_{ij} > 0$. For antiferromagnetics J is taken as negative for up and down spins, $J_{ij} < 0$.

3.1 Spin Waves in Ferromagnets

Ferromagnetic materials show a spontaneous magnetic moment also without an external magnetic field. In the ground state all (total) atomic spins are aligned parallel, and the magnetic and chemical unit cells are identical.

The z-component of a single spin S is $m_S = S$. Exciting this state, the z-component becomes reduced, $m_S < S$. In an energetically more favorable excitation state the excitations are distributed over all spins and the orientation of the spin vector relative to the lattice changes periodically forming a spin wave. The quantized particles of this spin wave are magnons.

In the Heisenberg-model the Hamiltonian of spins in an external magnetic field $\mathbf{B}$ can be written in the following way:

$$H = -\sum_{ij}{}' J_{ij} \mathbf{S}_i \cdot \mathbf{S}_j + \gamma \mu_B \mathbf{B} \cdot \sum_i \mathbf{S}_i. \tag{16}$$

The exchange integral J_{ij} decays fast with increasing distance between the atoms i and j, and in practice the interaction is limited to next neighbors. The second term is the Zeeman energy $-\mu_e \cdot \mathbf{B}$ which presents the potential energy of the spin magnetic moments with an external magnetic field $\mathbf{B}$; one typically chooses $\mathbf{B} = -B(0,0,1)$. The ions form a regular lattice, each

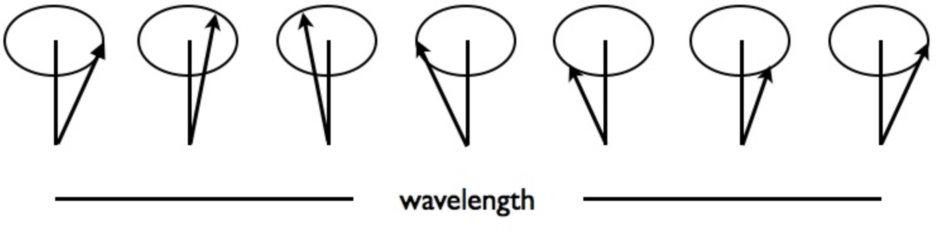

Fig. 9: *Schematic representation of a spin wave with wavelength* λ*.*

site is associated with a magnetic moment μ, with $\mu_e = -\gamma\mu_B\mathbf{S}_i/\hbar$, where γ is the Landé factor or gyromagnetic ratio ($\gamma \approx 2.00232$ for a single electron), μ_B is the Bohr magneton.

In general the Hamiltonian can contain further contributions, coming, e.g., from crystalline anisotropies coupling the spins to certain crystallographic directions, or the dipole-dipole interaction of the spins, etc. These contributions are usually smaller than the terms written down and shall be neglected.

We are now not dealing anymore with displacements (or creation and annihilation of displacement states) as in the phonon case but with creation and annihilation of magnon states. To describe excitations or the change in the z-component we introduce spin operators:

$$S_+\left|m\right\rangle \propto \left|m+1\right\rangle , \quad S_-\left|m\right\rangle \propto \left|m-1\right\rangle , \quad S_z\left|m\right\rangle = m\left|m\right\rangle \tag{17}$$

Note that $\mathbf{S}\cdot\mathbf{S} = \frac{1}{2}(S_+S_- + S_-S_+) + S_z^2$. The spin operators fulfill the commutation relations: $[S_+, S_-] = 2S_z$, $[S_z, S_\pm] = \pm S_\pm$.

To determine the eigenstates of (16) we relate the spin operators to Bose creation and annihilation operators $a^\dagger$ and a. This is the Holstein-Primakoff transformation. The spin operators can then be written as:

$$\begin{aligned} S_+^i &= S_x^i + iS_y^i = \sqrt{2S}\left(1 - \frac{a_i^\dagger a_i}{2S}\right)^{1/2} \cdot a_i, \\ S_-^i &= S_x^i - iS_y^i = \sqrt{2S}a_i^\dagger\left(1 - \frac{a_i^\dagger a_i}{2S}\right)^{1/2} = (S_+^i)^\dagger, \\ S_z^i &= S - a_i^\dagger a_i. \end{aligned} \tag{18}$$

The last equation describes the deviation from the maximum value S by the number operator $a_i^\dagger a_i$, which will turn out to be the quantized excitations. The commutation relations for the creation and annihilation operators are the same as they were in the phonon case.

As in the phonon case, we assume a periodic lattice. The Hamiltonian (16) is invariant against a translation of basis vectors within the lattice. This means, solutions of the equation of motion in plane wave form will exist, and we will make a Bloch ansatz as for lattice waves, equation (10). It is then convenient to let the creator and annihilators act on collective states given by the wavevector $\mathbf{q}$:

$$a_i = \frac{1}{\sqrt{N}}\sum_{\mathbf{q}} b_{\mathbf{q}} e^{-i\mathbf{q}\cdot\mathbf{R}^i} \text{ and } a_i^\dagger = \frac{1}{\sqrt{N}}\sum_{\mathbf{q}} b_{\mathbf{q}}^\dagger e^{i\mathbf{q}\cdot\mathbf{R}^i}. \tag{19}$$

The commutation relations for a_i and $a_i^\dagger$ are also valid for the $b_{\mathbf{q}}$ and $b_{\mathbf{q}}^\dagger$.

In the following we will consider low excitations with $S - m_S \ll S$. Similar to the harmonic approximation for the phonons where we expanded the potential only up to second order we will now only consider the lowest terms in a_i or $b_{\mathbf{q}}$. With this the square root in equation (18) is approximately $\left(1-\frac{a_i^\dagger a_i}{2S}\right)^{1/2} \approx 1$, and the spin operators result to:

$$\begin{aligned} S_+^i &= \sqrt{\frac{2S}{N}}\sum_{\mathbf{q}} b_{\mathbf{q}} e^{-i\mathbf{q}\cdot\mathbf{R}^i}, \\ S_-^i &= \sqrt{\frac{2S}{N}}\sum_{\mathbf{q}} b_{\mathbf{q}}^\dagger e^{i\mathbf{q}\cdot\mathbf{R}^i}, \\ S_z^i &= S-\frac{1}{N}\sum_{\mathbf{q}\mathbf{q}'} b_{\mathbf{q}}^\dagger b_{\mathbf{q}'} e^{i(\mathbf{q}-\mathbf{k}')\cdot\mathbf{R}^i}. \end{aligned} \tag{20}$$

These equations are of a similar type as the displacements in a lattice in the harmonic approximation. The applied approximation assumes small deviations of the spins from their original direction and thus only small excitation energies. This would be the case for small temperatures but the approximation has proven to be reasonable in many cases.

The solutions are thus collective wave-like states, which are the spin waves. In an analogy to the phonons, the quantized particles of these vibrations are called (ferromagnetic) magnons which are created and destroyed by the operators $b_{\mathbf{q}}^\dagger$, $b_{\mathbf{q}}$.

With the ansatz (20) in the Hamiltonian (16) and with the restriction to a Bravais lattice where $J_{ij} = J_{0,i-j}$ one assumes low excitations and truncates the expansion after second-order terms in $b_{\mathbf{q}}^\dagger$, $b_{\mathbf{q}}$. The Hamiltonian for spin waves in ferromagnets results to

$$H = E_0 + \hbar\omega(\mathbf{q})n_{\mathbf{q}} \quad \text{with} \quad n_{\mathbf{q}} = b_{\mathbf{q}}^\dagger b_{\mathbf{q}}. \tag{21}$$

with the ground-state energy depending on the interaction of the spins with an external magnetic field

$$E_0(B) = -NS^2 {\sum_{\mathbf{h}}}' J_{0\mathbf{h}} - \gamma\mu_B BNS \tag{22}$$

and the excitation energy

$$\hbar\omega(\mathbf{q}) = 4S\sum_{\mathbf{h}} J_{0\mathbf{h}}\sin^2(\mathbf{q}\cdot\mathbf{R}^{\mathbf{h}}/2) + \gamma\mu_B B \approx S\sum_{\mathbf{h}} J_{0\mathbf{h}}(\mathbf{q}\cdot\mathbf{R}^{\mathbf{h}})^2 + \gamma\mu_B B. \tag{23}$$

The result is valid with the assumption of small values of $\langle n_{\mathbf{q}}\rangle$ and neglects magnon-magnon interaction.

Equation (23) shows that the dispersion $\omega(\mathbf{q})$ is quadratic in q for small q, i.e. for long wavelengths. Unlike the case of phonons where $\omega(\mathbf{q})$ is linear in q for long wavelengths. The magnon dispersion is in the same energy range as the phonon dispersion, namely meV, see fig. 10.

Similar to a phonon dispersion the magnon dispersion can have several branches, e.g., different atoms in the magnetic unit cell or different sublattices can lead to not only one acoustic branch but additionally to one or several optic branches.

3.2 Spin Waves in Antiferromagnets

A simple model of an antiferromagnet assumes a lattice with two different sublattices with opposite spin directions like shown in fig. 3, where adjacent atoms belong to different sublattices. The total magnetization results to zero. An example is the lattice of the antiferromagnetic insulator MnF_2 crystal.

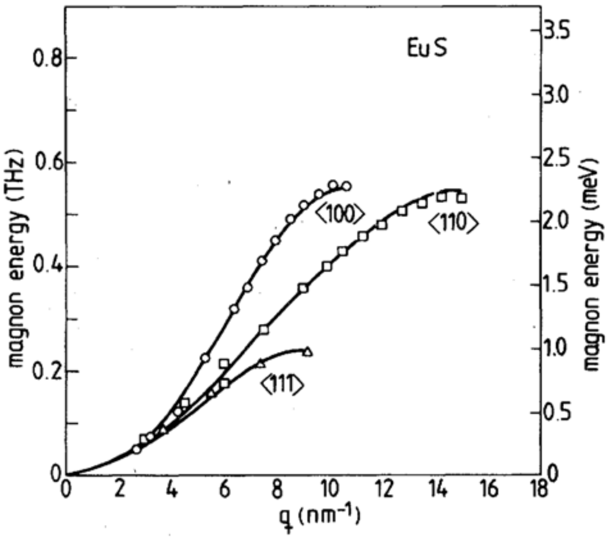

Fig. 10: *Magnon dispersion for ferromagnetic EuS from inelastic neutron scattering showing a strong anisotropy for different directions in* $\mathbf{q}$ *space. [7]*

The Hamiltonian has to include now the two different spin types, and the exchange integral is $J_{ij} < 0$ for an antiferromagnet. Like in the ferromagnet case we limit the interaction to next neighbors:

$$H = \sum_{ij} J_{ij} \mathbf{S}_1^i \cdot \mathbf{S}_2^j - \gamma \mu_B B \sum_i (\mathbf{S}_{1z}^i - \mathbf{S}_{2z}^j). \tag{24}$$

For simplicity, the Landé g-factor is assumed to be the same.

The following transformations are similar to the ferromagnet case, only one sort of spin (1) is aligned parallel to the z-direction, the other one antiparallel (2), as can be seen in the z-component of the spin operator. We employ again the Holstein-Primakoff transformation to replace the spin operators by boson operators. Now we have to take into account the two spin operators for the different sublattices. The equation equivalent to (18) is:

$$\begin{aligned} S_{1+}^i &= \sqrt{2S} \left(1 - \frac{a_{1i}^\dagger a_{1i}}{2S} \right)^{1/2} \cdot a_{1i}, \qquad (25) \\ S_{2+}^i &= \sqrt{2S} a_{2i}^\dagger \left(1 - \frac{a_{2i}^\dagger a_{2i}}{2S} \right)^{1/2}, \\ S_{1z}^i &= S - a_{1i}^\dagger a_{1i}, \quad S_{2z}^i = -S + a_{2i}^\dagger a_{2i} \end{aligned}$$

and $S_{1-}^i = (S_{1+}^i)^\dagger$, $S_{2-}^i = (S_{2+}^i)^\dagger$.

We perform the same transformation to operators in $\mathbf{q}$-space, equation (19), and the truncation of the expansion in $b_\mathbf{q}$,

$$H = E_0 + 2S \sum_\mathbf{h} J_{0,\mathbf{h}} \sum_\mathbf{q} \sum_{\sigma=1,2} b_{\mathbf{q}\sigma}^\dagger b_{\mathbf{q}\sigma} + 2S \sum_\mathbf{q} \sum_\mathbf{h} J_{0,\mathbf{h}} e^{i\mathbf{q}\cdot\mathbf{R^h}} (b_{\mathbf{q}1} b_{\mathbf{q}2} + b_{\mathbf{q}1}^\dagger b_{\mathbf{q}2}^\dagger). \tag{26}$$

The middle term counts elementary excitations on each sublattice. The last term contains cross-terms describing a coupling between two different sublattices. To finally diagonalize the Hamil-

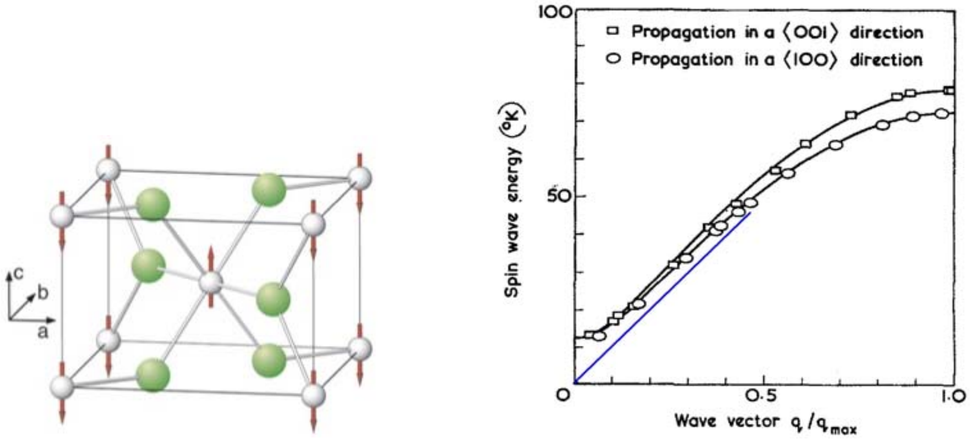

Fig. 11: *Left: Crystal and magnetic structure of MnF*$_2$*. The grey spheres represent Mn*$^{2+}$ *ions, the arrows their relative direction of spin. [8] Right: Magnon dispersion for two different directions in* k *space. [9]*

tonian this coupling has to be removed via a transformation called the Bogoliubov transformation:

$$b_{\mathbf{q}1} = u_{\mathbf{q}} c_{\mathbf{q}1} + v_{\mathbf{q}} c^{\dagger}_{\mathbf{q}2}, , \quad b_{\mathbf{q}2} = v_{\mathbf{q}} c^{\dagger}_{\mathbf{q}1} + u_{\mathbf{q}} c_{\mathbf{q}2}.$$

Here the magnon creators of one sublattice are related to annihilators in the other sublattice where the size of each part might vary with the substance under consideration.

The requirement that the new operators $c^\dagger$ and c be Bose creation and annihilation operators lead to $u^2_{\mathbf{q}} - v^2_{\mathbf{q}} = 1$. The resulting Hamiltonian contains terms with $c^\dagger c$ (as one expects), but also terms with two creation or annihilation operators, $c^\dagger c^\dagger$ and cc as in the last term in (26). The second requirement is the vanishing of the latter. This fixes the u and v and the final form of the Hamiltonian.

Finally the Hamiltonian for antiferromagnetic spin waves results to:

$$H = E_0 + \sum_{\mathbf{q}\sigma} \hbar\omega_{\mathbf{q}} \left(c^{\dagger}_{\mathbf{q}\sigma} c_{\mathbf{q}\sigma} + 1/2 \right). \tag{27}$$

Different from ferromagnetic magnons the Hamiltonian contains here the number operators of two elementary excitations with the same energy and a zero point contribution.

With the approximation for small q and $B = 0$:

$$\hbar\omega_{\mathbf{q}} \approx 2S \left(\sum_{\mathbf{h}} J_{0,\mathbf{h}} (\mathbf{q} \cdot \mathbf{R}^{\mathbf{h}})^2 \right)^{1/2}. \tag{28}$$

We see that in an antiferromagnet the dispersion $\omega(\mathbf{q})$ for small q or long wavelength is linear in q as it was for the phonon dispersion. As an example this linear dispersion measured by inelastic neutron scattering is shown in fig. 11. In this special case the dispersion does not follow the linear dispersion in q but exhibits a gap at $q = 0$. This is due to an anisotropy field, which removes the degeneracy of the two different magnons leading to a finite energy at $q = 0$.

3.3 Temperature Dependence of the Magnetization

Magnons can be thermally excited similar to phonons. Without external magnetic field and at very low temperatures we assume the magnetization $M(0) = g\mu_B NS$ saturated and all spins

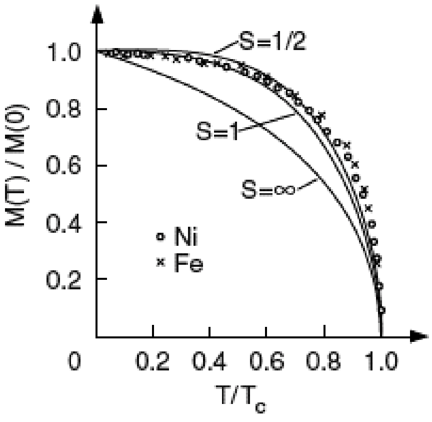

Fig. 12: *Reduced magnetization vs. reduced temperature for ferromagnetic Ni and Fe. The solid lines are calculations with different values for the total spin. [1]*

aligned. With increasing temperature the spontaneous magnetization $M(T)$ will decrease. We have seen before that the deviation from the saturated magnetization $M(0) \propto S$ is described by the occupation number operator $n_{\vec{q}}$.

In a ferromagnet the Curie temperature T_C separates the not-ordered paramagnetic phase, where the spontaneous magnetization vanishes, from the ordered ferromagnetic phase at $T < T_C$. The transition temperature for antiferromagnets is the Néel temperature T_N.

For temperatures below the Curie temperatures T_C the magnetization $M(T)$ for ferromagnets reads:

$$M(T) = \gamma\mu_B\Big(NS - \sum_{\mathbf{q}} \langle n_{\mathbf{q}} \rangle\Big), \tag{29}$$

where the brackets, $\langle \ldots \rangle$, denote the thermal average. The saturation magnetization of one sublattice in an antiferromagnet is smaller than NS, and not all spins are parallel but deviate from a perfect antiparallel spin alignment. The diminution depends e.g., on the type of lattice or structure. The term in brackets, is the total spin in the z-direction. For a cubic lattice with lattice constant a and small temperatures $T \ll T_C$ the relative deviation of the magnetization from its saturated value results to:

$$\frac{M(0) - M(T)}{M(0)} = \frac{2.315}{S} \frac{V}{4\pi^2 a^3} \left(\frac{k_B T}{2SJ}\right)^{3/2}. \tag{30}$$

This $T^{3/2}$-law of the spontaneous magnetization is also found experimentally, see fig. 12.

For an antiferromagnet in analogy to (29) the z-component of the magnetization of the first sublattice results to

$$M_1 = \gamma\mu_B\Big(NS - \sum_{\vec{k}} \langle b^\dagger_{\mathbf{q}1} b_{\mathbf{q}1} \rangle\Big) \tag{31}$$

The temperature dependence of the magnetization results in approximation for a cubic lattice to

$$\frac{M_1(0) - M_1(T)}{\gamma\mu_B} = \frac{V}{4\pi^2 a^3 \sqrt{2z}} \left(\frac{k_B T}{2JS}\right)^2. \tag{32}$$

(z is the number of neighbors.) Unlike in a ferromagnet the magnetization of an antiferromagnetic sublattice decreases with T^2 for small temperatures. The different temperature behavior is related to the different q-dependence of the dispersion curves at long wavelengths.

3.4 Dependence on magnetic field

So far we stated that in a ferromagnet at low temperatures well below T_C in general all magnetic moments are aligned parallel. Still one might find that the magnetization of the system increases in an applied magnetic field until reaching a saturation value. This is ascribed to the existence of domains, first postulated by P. Weiss (1907) and well established by now. In each of these domains the magnetization is saturated but oriented differently in respect to each other leading to lower total moment. The domain configuration might then change with an applied magnetic field. Within one domain however, one can expect to find well aligned spins, as the exchange interaction J_{ij} is short-range and limited to almost next-neighbors.
With applying an external magnetic field first the volume of the domains which are oriented already in direction of the external field will grow, then in a stronger external field, all domains will be oriented in direction of the external field.

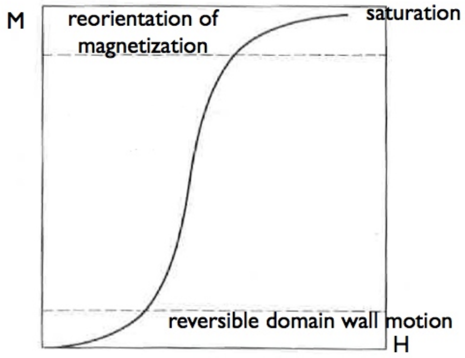

Fig. 13: *Schematic magnetization curve, magnetization vs. magnetic field.*

4 Conclusion

As a conclusion we have seen here the formalism for elementary excitations for lattice and spin waves or respectively their quasiparticles phonons and magnons.
We saw first that we can decouple the electron from the ion dynamics and that it's enough to treat the ion movement in a potential V. The second major approximation was the truncation of this potential after the second order term. This allowed a harmonic ansatz for the displacements leading to a set of uncoupled harmonic oscillators / collective modes. Assuming an infinite periodic crystal the equations could be simplified and it was sufficient to look only at the dynamics within one unit cell or the first Brillouin zone. From the equations of motions the dynamical matrix and frequencies and eigenvectors and finally the dispersion curves resulted. For small q the acoustic-mode dispersion is linear in q approaching the velocity of sound. The phonon spectrum can also be presented with the phonon density of states . For temperature dependent effects higher order terms in the potential expansion have to be taken into account.
In case of amorphous materials, where the lattice periodicity is more or less missing, the short range order still leads to a phonon dispersion at small **q** vectors.

We treated the spin waves in a similar formalism as the lattice waves. Within the Heisenberg-model we determined the eigenstates with relating the spin operators to the creation and annihilation operators (Holstein-Primakoff transformation). Only that instead of creating or annihilating displacement states we were dealing now with magnon states. For an infinite periodic lattice we could make a Bloch ansatz for plane waves as for the phonons. And similar to the harmonic approximation where we expanded the potential only up to second order we considered only lowest terms in the creation and annihilation operators. In ferromagnets the spin wave dispersion curves were found to be quadratic in q, in antiferromagnets linear in q. The formalism for antiferromagnets differs from the one for ferromagnets as one has to consider two different spin-sublattices. This calls for another transformation called the Bogoliubov transformation, necessary to decouple the sublattices and be able to diagonalize the Hamiltonian.

In general the magnetization vanishes with increasing temperature. The transition temperature is called Curie- and Néel temperature for ferro- and antiferromagnets. The formalism presented was based in general on the assumption of having only one magnetic domain. In reality many domains might exist in a sample, leading to an increase of magnetization in external magnetic field.

References

[1] Textbooks on Solid State Physics:

W. Ludwig, *Festkörperphysik II* (Akademische Verlagsgesellschaft Frankfurt am Main 1970)
U. Rössler, *Solid State Theory: An Introduction* (Physica Verlag, Springer, Berlin Heidelberg 2009)

[2] A. A. Maradudin, E. W. Montroll, G. H. Weiss, I. P. Ipatova, *Theory of lattice dynamics in the harmonic approximation, Solid State Phys.: Advances in research and application* (Academic Press, 2^{nd} Ed, 1971)

[3] A. A. Quong, B. M. Klein, Phys. Rev. B **46**, 10734 (1992).

[4] K. Schmalzl, D. Strauch, H. Schober, Phys. Rev. B **68**, 144301 (2003)

[5] M. T. Dove, *Introduction to Lattice Dynamics* (Cambridge University Press, 1993)

[6] L. Orsingher, G. Baldi, A. Fontana, L. E. Bove, T. Unruh, A. Orecchini, C. Petrillo, N. Violini, F. Sacchetti, Phys. Rev. B **82**, 115201 (2010)

[7] H. G. Bohn, W. Zinn, B. Dorner, A. Kollmar, Phys. Rev B **22**, 5447 (1980)

[8] S. P. Bayrakci, T. Keller, K. Habicht, B. Keimer, Science **312**, 1926 (2006)

[9] G. G. Low, A. Okazaki, R. W. H. Stevenson, K. C. Turberfield, J. appl. Phys. **35**, 998 (1964)